Nonperturbative renormalization group for the Landau–de Gennes model

Bin Qin,[1,*] Defu Hou,[1,†] Mei Huang,[2,‡] Danning Li,[3,§] and Hui Zhang[1,4,‖]

[1]*Institute of Particle Physics (IOPP) and Key Laboratory of Quark and Lepton Physics (MOE), Central China Normal University, Wuhan 430079, China*

[2]*Institute of High Energy Physics, Chinese Academy of Sciences, Beijing 100049, China*

[3]*Department of Physics and Siyuan Labotorary, Jinan University, Guangzhou 510632, China*

[4]*Physics Department and Center for Exploration of Energy and Matter, Indiana University, 2401 N Milo B. Sampson Lane, Bloomington, Indiana 47408, USA*

(Received 3 March 2018; published 3 July 2018)

We study the nematic isotropic phase transition by applying the functional renormalization group to the Landau–de Gennes model. We derive the flow equations for the effective potential as well as the "couplings" constants and the anomalous dimension. We then solve the coupled flow equations on a grid using the Newton-Raphson method. A first-order phase transition is observed. We also investigate the nematic isotropic puzzle (the NI puzzle) in this paper. We obtain the NI transition temperature difference $T_c - T^* = 5.85$ K.

DOI: 10.1103/PhysRevB.98.014102

I. INTRODUCTION

The nematic isotropic (NI) phase transition has been an important topic of research over the past few decades [1–3]. In uniaxial nematic liquid crystals the centers of gravity of the molecules have no long-range order while all their axes point in roughly the same direction, described by the director, around which there exists complete rotational symmetry. When raising temperature, its order parameter abruptly drops to zero and becomes an isotropic phase. Thus the NI phase transition is of first order in nature. It can be described phenomenologically by the mean-field Landau scalar model with a cubic term [1]. But it is relatively weak because only orientational order is lost and the latent heat is small [3]. This also leads to large pretransition anomalies such as specific heat, which indicates that the transition is close to being second order. In the isotropic phase, although the order parameter vanishes on average, the molecules are still parallel to each other over a characteristic distance (the correlation length) which describes the average size of the range of correlations between the molecules. This means that fluctuation effects should play a role in the physics of liquid crystals.

Drozd-Rzoska *et al.* found that the temperature behavior of dielectric permittivity in the isotropic phase of nematogens could be described in the same way as in critical binary solutions. This fluidlike analogy was also applied to the nonlinear dielectric effect, which describes changes of dielectric permittivity induced by a strong electric field [4]. They also found evidence for the equivalence of temperature and pressure paths on approaching the NI phase transition through high-pressure, isothermal studies of the low-frequency nonlinear dielectric effect in the isotropic phase of nematogens, which makes it possible to investigate the pretransitional effects under high pressure from temperature measurements carried out under atmospheric pressure [5]. Rzoska *et al.* studied the singular behavior of the static dielectric permittivity of nematogens below and above NI phase-transition temperature. The derivative of experimental data (e.g., the mean value of the nematic permittivity) with respect to temperature shows the specific-heat-like behavior with universal exponents. They confirmed the hypothesis of the fluidlike, pseudospinodal, and tricritical behavior of the NI phase transition [6]. Syed *et al.* also found evidence for tricritical behavior of a cyclic liquid crystalline trimer [7]. Simões *et al.* showed that the nematic order parameter presents a singular universal behavior that is not restricted to the neighborhoods of the NI phase transition, but encompasses the entire range of the nematic phase independent of what is the actual phase or mesophase bordering the nematic phase at low temperatures [8,9].

Since fluctuation effects play such an important role, many attempts had been made to take them into account. de Gennes proposed a tensor order-parameter model, denoted the Landau–de Gennes model [1,10]. Wang *et al.* investigated the influence of fluctuations on critical and multicritical behavior of nematic liquid crystals in this model, but their treatment is limited to the harmonic approximation [11]. This model also gains insight into the long-standing puzzle about the low value of $\frac{T_c - T^*}{T^*} \approx 0.1\%$, where T_c is the nematic-isotropic phase-transition temperature and T^* is interpreted as the temperature at which the light-scattering intensity diverges in the supercooled isotropic phase. In experiments, it is shown that $T_c - T^* \approx 1K$ ($\frac{T_c - T^*}{T^*} \approx 0.3\%$) in the case of nematic liquid crystal 8CB, which is much smaller than the usual theoretical model predictions. For instance the mean-field result gives $T_c - T^* = 24$ K. Tao *et al.* extended the mean-field theory by including the isotropic, density dependent component of the molecular interaction, and their result showed accordance with the experimental values. However, they

*qinbin@mails.ccnu.edu.cn
†houdf@mail.ccnu.edu.cn
‡huangm@ihep.ac.cn
§lidanning@jnu.edu.cn
‖Mr.zhanghui@mails.ccnu.edu.cn

neglected the influence of fluctuations [12]. By including fluctuations and using Wilson's renormalization-group analysis, Mukherjee *et al.* got the result $T_c - T^* = 7.47$ K and further obtained $T_c - T^* = 3$ K, which remains the best result today in those works that have considered the effects of fluctuations [10,13–15].

The nonperturbative renormalization group (NPRG, also called the functional renormalization group, or FRG) [16] has been proven to be an extremely versatile and efficient tool to deal with fluctuations in recent years [17–29]; see [25–29] for an excellent introduction. With this method one can systematically extract quantitative reliable results about long-distance physics from short-distance ansatz. As opposed to the usual functional integral approach in field theory, its conceptual framework is relatively simple and unified, and essentially takes the form of functional differential equations which are more convenient for numerical computations. So the goal of this paper is to solve the Landau–de Gennes model using the methods of nonperturbative renormalization group and investigate the NI puzzle in this framework.

The paper is organized as follows. In Sec. II, we define the model and notations. Then we give a quick overview of the FRG formalism and apply it to the model. The concrete flow equations are derived, including the anomalous dimension. In Sec. III, we show our numerical results about effective potential. We also give our analysis of the nematic-isotropic puzzle. In Sec. IV we give our concluding remarks and outlook for future work.

II. APPLICATION OF NONPERTURBATIVE RENORMALIZATION GROUP TO THE LANDAU–DE GENNES MODEL

The Lagrangian density of the Landau-de Gennes model can be written as [10,13]

$$L = \tfrac{1}{2}A\,\mathrm{Tr}[Q^2] + \tfrac{1}{3}B\,\mathrm{Tr}[Q^3] + \tfrac{1}{4}C\,\mathrm{Tr}[Q^4] + \mathrm{Tr}(\nabla Q)^2\,. \tag{1}$$

In the most general sense Q is a symmetric traceless second rank tensor, which vanishes in the symmetric isotropic phase, and presents a finite value in the ordered nematic phase. In this paper, we parametrize Q as

$$Q = \frac{1}{\sqrt{2}}\begin{pmatrix} -\frac{\psi_1}{\sqrt{3}} - \psi_2 & \psi_3 & \psi_4 \\ \psi_3 & \psi_2 - \frac{\psi_1}{\sqrt{3}} & \psi_5 \\ \psi_4 & \psi_5 & \frac{2\psi_1}{\sqrt{3}} \end{pmatrix}, \tag{2}$$

where $\psi_1, \ldots, \psi_5$ are scalar fields.

The central concept of the NPRG formalism is the scale dependent effective average action Γ_k. The evolution of Γ_k with respect to the scale obeys an exact flow equation, the Wetterich equation:

$$\partial_k \Gamma_k[\psi_1, \ldots, \psi_5] = \frac{1}{2}\mathrm{Tr}\int d^D q\, \partial_k R_k(q^2)\big\{\Gamma_k^{(2)}[q, -q, \psi_1, \ldots, \psi_5] + R_k(q^2)\big\}^{-1}, \tag{3}$$

where $\Gamma_k^{(2)}[q, -q, \psi_1 \ldots \psi_5]$ is the Fourier transform of the second functional derivatives of Γ_k:

$$\Gamma_{k,mn}^{(2)}[x, y, \psi_1, \ldots, \psi_5] = \frac{\delta\Gamma_k[\psi_1, \ldots, \psi_5]}{\delta\psi_m(x)\delta\psi_n(y)}. \tag{4}$$

where $m, n = 1, \ldots, 5$. The initial condition $\Gamma_{k=k_0}$ at the scale k_0 is given by the classical action.

$R_k(q^2)$ is the Litim regulator [30]:

$$R_k(q^2) = Z_k(k^2 - q^2)\Theta(k^2 - q^2)\,, \tag{5}$$

where Z_k is the running wave function renormalization and Θ is the usual step function.

The Lagrangian density can be expanded in terms of two basic invariants:

$$\begin{aligned} \rho &= \mathrm{Tr}[Q^2] = \psi_1^2 + \psi_2^2 + \psi_3^2 + \psi_4^2 + \psi_5^2\,, \\ \tau &= \mathrm{Tr}[Q^3] = \frac{1}{6\sqrt{2}}\big(2\sqrt{3}\psi_1^3 - 9\psi_2\psi_4^2 + 9\psi_2\psi_5^2 + 18\psi_3\psi_4\psi_5 \\ &\quad + 3\sqrt{3}\psi_1\big(-2\psi_2^2 - 2\psi_3^2 + \psi_4^2 + \psi_5^2\big)\big). \end{aligned} \tag{6}$$

There exists an interesting property for these two invariants, which will be quite useful in the following calculations:

$$6\tau^2 - \rho^3 = -\big(\psi_2^3 - 3\psi_1^2\psi_2\big)^2 \leqslant 0. \tag{7}$$

For the Landau–de Gennes model we consider the following simplified effective average action:

$$\Gamma_k = \int d^D x\{U_k(\rho, \tau) + Z_k[(\partial\psi_1)^2 + \cdots + (\partial\psi_5)^2]\}. \tag{8}$$

The flow equation for the effective average potential follows from its definition:

$$U_k(\rho, \tau) = \frac{1}{\Omega}\Gamma_k[\Phi], \tag{9}$$

where Ω is the volume of the system and Φ is a constant field configuration, which is obtained by setting the fluctuating field Q matrix elements as constants. Since Φ is symmetric, we can always find a frame of reference to diagonalize it. We denote the diagonal form of the physical equilibrium configuration Φ simply as Φ_{diag},

$$\Phi_{\mathrm{diag}} = \frac{1}{\sqrt{2}}\begin{pmatrix} -\frac{\phi_1}{\sqrt{3}} - \phi_2 & 0 & 0 \\ 0 & \phi_2 - \frac{\phi_1}{\sqrt{3}} & 0 \\ 0 & 0 & \frac{2\phi_1}{\sqrt{3}} \end{pmatrix}, \tag{10}$$

where ϕ_1 and ϕ_2 are constants.

There also exists a microscopic description of the liquid crystals, the simplest of which are rigid rods. Taking the z axis of laboratory frame as the axis of ordering, the order parameter reads

$$Q^M = S\begin{pmatrix} -\frac{1}{3} & 0 & 0 \\ 0 & -\frac{1}{3} & 0 \\ 0 & 0 & \frac{2}{3} \end{pmatrix}, \tag{11}$$

while in an arbitrary frame of reference:

$$Q^M_{\alpha\beta} = S\big(n_\alpha n_\beta - \tfrac{1}{3}\delta_{\alpha\beta}\big)\,, \tag{12}$$

where $S = \frac{3}{2}\langle\cos^2\theta\rangle - \frac{1}{2}$, $\hat{n}$ describes the average direction of the alignment of molecules (i.e., the direction of the nematic

axis). Q^M is equal to Eq. (10) provided $\phi_2 = 0$, $\phi_1 = \sqrt{\frac{2}{3}}S$. Since by definition S and Q are dimensionless, the coefficient before the kinetic term in Eqs. (1) and (8) has dimension k^{D-2}, and A, B, C have dimension k^D.

In the field configuration Φ_{diag} the two basic invariants ρ and τ read

$$\phi_1^2 + \phi_2^2 = \rho\,, \tag{13}$$

$$\frac{\phi_1(\phi_1^2 - 3\phi_2^2)}{\sqrt{6}} = \tau\,. \tag{14}$$

We can then solve the field in terms of the invariants

$$\phi_1 = -\frac{1}{2}\left(\frac{\sqrt[3]{\sqrt{36\tau^2 - 6\rho^3} - 6\tau}}{\sqrt[6]{6}} + \frac{\sqrt[6]{6}\rho}{\sqrt[3]{\sqrt{36\tau^2 - 6\rho^3} - 6\tau}}\right), \tag{15}$$

$$\phi_2 = -\frac{1}{2\sqrt{6}}\sqrt{-(6\sqrt{36\tau^2 - 6\rho^3} - 36\tau)^{2/3} - \frac{6\sqrt[3]{6}\rho^2}{(\sqrt{36\tau^2 - 6\rho^3} - 6\tau)^{2/3}} + 12\rho}\,. \tag{16}$$

There are also five other solutions, but each of them leads to the same final flow equations. Note that the property Eq. (7) can be used to transform the solution into complex functions. For example

$$\sqrt{36\tau^2 - 6\rho^3} - 6\tau = -\sqrt{6}\rho^{\frac{3}{2}}\exp\left[-i\tan^{-1}\left(\frac{\sqrt{\rho^3 - 6\tau^2}}{\sqrt{6}\tau}\right)\right]. \tag{17}$$

When we substitute the complex function back to the solutions, the imaginary parts all exactly cancel out, leaving the real part, as it should be, for example,

$$\phi_1 = -\sqrt{\rho}\sin\left[\frac{1}{3}\tan^{-1}\left(\frac{\sqrt{\rho^3 - 6\tau^2}}{\sqrt{6}\tau}\right) + \frac{\pi}{6}\right], \quad \phi_2 = -\frac{1}{\sqrt{2}}\sqrt{\rho\sin\left[\frac{\pi}{6} - \frac{2}{3}\tan^{-1}\left(\frac{\sqrt{\rho^3 - 6\tau^2}}{\sqrt{6}\tau}\right)\right] + \rho}\,. \tag{18}$$

Then we can calculate all the two-point vertices (and the propagator matrix as its inverse) and three-point vertices term by term. The flow equation for the potential reads

$$\frac{\partial U_k(\rho,\tau)}{\partial k} = \frac{k^{D-1}K_D}{D}Z_k k^2\left(1 - \frac{\eta_k}{D+2}\right)\left(\Sigma_{i=1}^5 \frac{1}{Z_k k^2 + M_i^2}\right), \tag{19}$$

where $K_D = \frac{1}{2^{D-1}\pi^{D/2}\Gamma(D/2)}$; the running anomalous dimension is defined by

$$\eta_k = -\frac{k}{Z_k}\frac{\partial Z_k}{\partial k} \tag{20}$$

and the mass eigenvalues are given by

$$M_1^2 = \frac{1}{2}\left[\sqrt{\rho}\left(3\sqrt{\cos\left(\frac{\alpha}{3}\right) + 1} - \sqrt{6}\sin\left(\frac{\alpha}{6}\right)\right)U_k{}^{(0,1)}(\rho,\tau) + 4U_k{}^{(1,0)}(\rho,\tau)\right], \tag{21}$$

$$M_2^2 = \frac{1}{2}\left[-\sqrt{\rho}\left(3\sqrt{\cos\left(\frac{\alpha}{3}\right) + 1} + \sqrt{6}\sin\left(\frac{\alpha}{6}\right)\right)U_k{}^{(0,1)}(\rho,\tau) + 4U_k{}^{(1,0)}(\rho,\tau)\right], \tag{22}$$

$$M_3^2 = \sqrt{6\rho}\sin\left(\frac{\alpha}{6}\right)U_k{}^{(0,1)}(\rho,\tau) + 2U_k{}^{(1,0)}(\rho,\tau), \tag{23}$$

$$M_4^2 = p - \frac{\sqrt{q}}{4} \quad , \quad M_5^2 = p + \frac{\sqrt{q}}{4}, \tag{24}$$

where $\alpha = 2\tan^{-1}\left(\frac{\sqrt{\rho^3 - 6\tau^2}}{\sqrt{6}\tau}\right) + \pi$, and

$$p = \tfrac{3}{4}\rho^2 U_k{}^{(0,2)}(\rho,\tau) + 2\rho U_k{}^{(2,0)}(\rho,\tau) + 2U_k{}^{(1,0)}(\rho,\tau) + 6\tau U_k{}^{(1,1)}(\rho,\tau), \tag{25}$$

$$\begin{aligned} q = {} & 96\rho U_k{}^{(0,1)}(\rho,\tau)^2 + 48\left[4\rho^2 U_k{}^{(1,1)}(\rho,\tau) + 3\rho\tau U_k{}^{(0,2)}(\rho,\tau) + 8\tau U_k{}^{(2,0)}(\rho,\tau)\right]U_k{}^{(0,1)}(\rho,\tau) \\ & + \rho\left(48\rho U_k{}^{(0,2)}(\rho,\tau)\left\{\rho U_k{}^{(2,0)}(\rho,\tau)\cos\left[2\tan^{-1}\left(\frac{\sqrt{\rho^3 - 6\tau^2}}{\sqrt{6}\tau}\right)\right] + 3\tau U_k{}^{(1,1)}(\rho,\tau)\right\}\right. \\ & \left. + 9\rho^3 U_k{}^{(0,2)}(\rho,\tau)^2 + 32\left(3\rho^2 U_k{}^{(1,1)}(\rho,\tau)^2 + 12\tau U_k{}^{(2,0)}(\rho,\tau)U_k{}^{(1,1)}(\rho,\tau) + 2\rho U_k{}^{(2,0)}(\rho,\tau)^2\right)\right). \end{aligned} \tag{26}$$

It is often convenient to work with dimensionless renormalized quantities that are defined by

$$\tilde{\rho} = Z_k k^{2-D}\rho, \quad \tilde{\tau} = (Z_k k^{2-D})^{3/2}\tau, \quad \tilde{U}_t(\tilde{\rho},\tilde{\tau}) = k^{-D}U_k(\rho,\tau). \tag{27}$$

We define a new scale $t = -\ln\frac{k}{k_0}$ (following the convention of [25]), which is called the RG time. The flow equation for the dimensionless potential reads

$$\begin{aligned}\frac{\partial\tilde{U}_t(\tilde{\rho},\tilde{\tau})}{\partial t} &= \tilde{\rho}(-D-\eta_t\tilde{\rho}+2)\frac{\partial\tilde{U}_t(\tilde{\rho},\tilde{\tau})}{\partial\tilde{\rho}} + \frac{3}{2}\tilde{\tau}(-D-\eta_t\tilde{\tau}+2)\frac{\partial\tilde{U}_t(\tilde{\rho},\tilde{\tau})}{\partial\tilde{\tau}} + D\tilde{U}_t(\tilde{\rho},\tilde{\tau}) \\ &\quad - \frac{K_D}{D}\left(1-\frac{\eta_t}{D+2}\right)\left(\frac{1}{m_1^2+1}+\frac{1}{m_2^2+1}+\frac{1}{m_3^2+1}+\frac{1}{m_4^2+1}+\frac{1}{m_5^2+1}\right),\end{aligned} \tag{28}$$

where m_i^2 are the dimensionless counterparts of M_i^2.

This is the full equation for the potential. But it is extremely difficult to solve directly due to its complexity. In order to extract useful physics from it, we make the following approximations. To simplify the notation we introduce

$$\epsilon(\tilde{\rho}) = \tilde{U}_t[\tilde{\rho},\tilde{\tau}=0], \tag{29}$$

$$\epsilon'(\tilde{\rho}) = \tilde{U}_t{}^{(1,0)}[\tilde{\rho},\tilde{\tau}=0], \tag{30}$$

$$\lambda(\tilde{\rho}) = 3\tilde{U}_t{}^{(0,1)}[\tilde{\rho},\tilde{\tau}=0]. \tag{31}$$

For $n \geqslant 2$, we set $\tilde{U}_t{}^{(0,n)}[\tilde{\rho},\tilde{\tau}=0]=0$, then $\tilde{U}_t(\tilde{\rho},\tilde{\tau})$ can be expressed as

$$\tilde{U}_t(\tilde{\rho},\tilde{\tau}) = \tfrac{1}{3}\tilde{\tau}\lambda(\tilde{\rho}) + \epsilon(\tilde{\rho}). \tag{32}$$

The scale dependence of ϵ is given by

$$\begin{aligned}\frac{\partial\epsilon}{\partial t} &= D\epsilon - D\tilde{\rho}\epsilon' - \tilde{\rho}\eta_t\epsilon' + 2\tilde{\rho}\epsilon' - \frac{K_D}{D}\left(1-\frac{\eta_t}{D+2}\right)\left(\frac{1}{2\epsilon'+1} + \frac{8\epsilon'+4}{-\lambda^2\tilde{\rho}+8\epsilon'^2+8\epsilon'+2}\right. \\ &\quad \left. + \frac{6(2\tilde{\rho}\epsilon''+2\epsilon'+1)}{-2\lambda^2\tilde{\rho}-2\tilde{\rho}^3\lambda'^2-4\lambda\tilde{\rho}^2\lambda'+12\tilde{\rho}\epsilon''+12\epsilon'(2\tilde{\rho}\epsilon''+1)+12\epsilon'^2+3}\right).\end{aligned} \tag{33}$$

Similarly for λ one finds

$$\begin{aligned}\frac{\partial\lambda}{\partial t} &= D\lambda - 3\tilde{\rho}\lambda'(D+\eta_t-2) - \frac{3}{2}\lambda(D+\eta_t-2) - \frac{K_D}{D}\left(1-\frac{\eta_t}{D+2}\right)\left(\frac{4(\lambda-6\tilde{\rho}\lambda')(\lambda^2\tilde{\rho}+8\epsilon'^2+8\epsilon'+2)}{\tilde{\rho}(-\lambda^2\tilde{\rho}+8\epsilon'^2+8\epsilon'+2)^2}\right. \\ &\quad + \frac{4(\tilde{\rho}\lambda''+4\lambda')}{-2\lambda^2\tilde{\rho}-2\tilde{\rho}^3\lambda'^2-4\lambda\tilde{\rho}^2\lambda'+12\tilde{\rho}\epsilon''+12\epsilon'(2\tilde{\rho}\epsilon''+1)+12\epsilon'^2+3} - \frac{2(3\tilde{\rho}\lambda'+\lambda)}{\tilde{\rho}(2\epsilon'+1)^2} \\ &\quad \left. - \frac{12(\sqrt{2}\tilde{\rho}^{3/2}\lambda'+\lambda\sqrt{2\tilde{\rho}}-2\tilde{\rho}\epsilon'')[\epsilon''(2\tilde{\rho}\lambda'-6\lambda)+(2\epsilon'+1)(\tilde{\rho}\lambda''+4\lambda')]}{[-2\lambda^2\tilde{\rho}-2\tilde{\rho}^3\lambda'^2-4\lambda\tilde{\rho}^2\lambda'+12\tilde{\rho}\epsilon''+12\epsilon'(2\tilde{\rho}\epsilon''+1)+12\epsilon'^2+3]^2}\right).\end{aligned} \tag{34}$$

The evolution equation for its derivative $\epsilon'(\tilde{\rho})$ can also be calculated analogously:

$$\begin{aligned}\frac{\partial\epsilon'}{\partial t} &= D\epsilon' - \tilde{\rho}\epsilon''(D+\eta_t-2) - \epsilon'(D+\eta_t-2) - \frac{K_D}{D}\left(1-\frac{\eta_t}{D+2}\right)\left(\frac{4\lambda(2\epsilon'+1)(2\tilde{\rho}\lambda'+\lambda)-8\epsilon''(\lambda^2\tilde{\rho}+2(2\epsilon'+1)^2)}{[\lambda^2\tilde{\rho}-2(2\epsilon'+1)^2]^2}\right. \\ &\quad + \frac{12(\tilde{\rho}\epsilon'''+2\epsilon'')}{-2\lambda^2\tilde{\rho}-2\tilde{\rho}^3\lambda'^2-4\lambda\tilde{\rho}^2\lambda'+12\tilde{\rho}\epsilon''+12\epsilon'(2\tilde{\rho}\epsilon''+1)+12\epsilon'^2+3} - \frac{2\epsilon''}{(2\epsilon'+1)^2} \\ &\quad \left. - \frac{12(2\tilde{\rho}\epsilon''+2\epsilon'+1)\{-2\lambda\tilde{\rho}(\tilde{\rho}\lambda''+3\lambda')+12\tilde{\rho}\epsilon'^2+\tilde{\rho}[6(2\epsilon'+1)\epsilon'''-\tilde{\rho}\lambda'(2\tilde{\rho}\lambda''+5\lambda')]-\lambda^2+12(2\epsilon'+1)\epsilon''\}}{[-2\lambda^2\tilde{\rho}-2\tilde{\rho}^3\lambda'^2-4\lambda\tilde{\rho}^2\lambda'+12\tilde{\rho}\epsilon''+12\epsilon'(2\tilde{\rho}\epsilon''+1)+12\epsilon'^2+3]^2}\right).\end{aligned} \tag{35}$$

It is worth noting that if our only objective is to get the above simplified equations rather than the full machinery, we can also circumvent the substitution technique, and set $\tilde{\tau}=0$ directly at last. We have verified that these two approaches indeed lead to the same equations.

Z_k can be extracted from the flow equation through

$$Z_k = \frac{(2\pi)^D}{\delta(0)}\lim_{p^2\to 0}\frac{\mathrm{d}}{\mathrm{d}p^2}\left(\frac{\partial^2\Gamma_k}{\delta\psi_m(p)\delta\psi_n(-p)}\right). \tag{36}$$

Without loss of generality we take $m=4$ and $n=4$ in this paper.

It can be shown that

$$\eta_k = \frac{k^{D+2}K_D}{DZ_k}\Sigma[Z_k\delta_{ab}G_{bc}\Gamma_{cdn}G_{di}Z_k\delta_{ij}G_{je}\Gamma_{efm}G_{fa}],$$

where G_{bc} is the propagator matrix element, and the propagator matrix is defined by the inverse of the two-point vertex. Γ_{cdn} is the three-point vertex.

We then express η_k in terms of dimensionless variables and finally get

$$\eta_t = \frac{K_D}{D}\left(\frac{4\lambda^2}{(\lambda^2\tilde{\rho}-8\epsilon'^2-8\epsilon'-2)^2}+\frac{24(2\lambda\tilde{\rho}\lambda'+\tilde{\rho}^2\lambda'^2+\lambda^2-3\epsilon''-6\epsilon'\epsilon'')}{(2\lambda^2\tilde{\rho}+2\tilde{\rho}^3\lambda'^2+4\lambda\tilde{\rho}^2\lambda'-12\tilde{\rho}\epsilon''-24\tilde{\rho}\epsilon'\epsilon''-12\epsilon'^2-12\epsilon'-3)^2}\right.$$
$$\left.-\frac{4(-2\lambda\tilde{\rho}\lambda'-\tilde{\rho}^2\lambda'^2-\lambda^2+6\epsilon''+12\epsilon'\epsilon'')}{(2\epsilon'+1)^2(2\lambda^2\tilde{\rho}+2\tilde{\rho}^3\lambda'^2+4\lambda\tilde{\rho}^2\lambda'-12\tilde{\rho}\epsilon''-24\tilde{\rho}\epsilon'\epsilon''-12\epsilon'^2-12\epsilon'-3)}\right). \quad (37)$$

When $\lambda = 0$ and evaluated at the minimum $\tilde{\rho}_0$ [i.e., $\epsilon'(\tilde{\rho}_0) = 0$] this reduces to

$$\eta_t = \frac{32\tilde{\rho}_0 K_D \epsilon''^2}{D(4\tilde{\rho}_0\epsilon''+1)^2}, \quad (38)$$

which is identical to the usual $O(5)$ model expression, if considering the different definition of ρ.

III. NUMERICAL RESULTS

We solve the combined equations (34) and (36) together [31] by discretizing the differential equations in this form:

$$\frac{u_i(t')-u_i(t)}{\Delta t} = F\left(u_i(t'),u_i^{(1)}(t'),u_i^{(2)}(t')\right), \quad (39)$$

where $t' = t+\Delta t$, $u_i(t)$ (i from 1 to n) denotes $\epsilon'(\tilde{\rho})$, $u_i(t)$ (i from $n+1$ to $2n$) denotes $\lambda(\tilde{\rho})$, and F is the discretized right-hand side of the combined equations. To evaluate the derivatives on the right-hand side six-point formulas are used. We take 60 points for the discretization of the variable (i.e., $n = 60$) and solve these nonlinear algebraic equations using the Newton-Raphson algorithm. The basic idea is to set the previous solution as the trial solution and search for the next step solution with the aid of Jacobian many times until the necessary accuracy is achieved.

We solve the above equation for the first few steps, and then switch to the following equation to improve its accuracy:

$$\frac{1}{12\Delta t}\{25u_i(t')-48u_i(t)+36u_i(t-\Delta t)-16u_i(t-2\Delta t)$$
$$+3u_i(t-3\Delta t)\} = F\left(u_i(t'),u_i^{(1)}(t'),u_i^{(2)}(t')\right). \quad (40)$$

It is convenient to define $\kappa = -\frac{A}{C}$ and rewrite the initial potential as

$$U(\rho,\tau) = \frac{B\tau}{3}+\frac{1}{4}C(\rho-\kappa)^2 = \frac{B\tau}{3}+\frac{C\kappa^2}{4}$$
$$-\frac{C\kappa\rho}{2}+\frac{C\rho^2}{4}, \quad (41)$$

differing by an irrelevant constant term. For specific values of the parameters, we first get the evolution result for $\epsilon'(\tilde{\rho})$ [$\epsilon(\tilde{\rho})$ can be calculated through direct integration] and $\lambda(\tilde{\rho})$. We then transform back to the original unscaled variables. To get the physical effective potential, we project our solution to the branch $\phi_2 = 0$, then $\rho = \phi_1^2$, $\tau = \frac{\phi_1^3}{\sqrt{6}}$, i.e., $\tau = \frac{\rho^{3/2}}{\sqrt{6}}$, which can be used to eliminate τ. Combining with Eqs. (32) and (27), we can obtain U_k as a function of ρ and define $\phi = \sqrt{\rho}$ to denote the resulting effective average potential as

$$W_t(\phi) = \frac{k^D}{3}(Z_k k^{2-D})^{3/2}\frac{\phi^3}{\sqrt{6}}\lambda(Z_k k^{2-D}\phi^2)$$
$$+k^D\epsilon(Z_k k^{2-D}\phi^2). \quad (42)$$

When $B = 0$, the Landau–de Gennes model reduces to the $O(5)$ model, as can be clearly seen from the Lagrangian density Eq. (1). This can also be verified numerically. When B is initially zero, it is observed that for arbitrary values of C and κ the cubic "coupling" λ always stays zero in the flow process and ϵ exhibits the same behavior as in the $O(5)$ model. Then we turn on the explicit symmetry breaking term. Since Landau–de Gennes model is a purely phenomenological theory, it is quite difficult to determine the coefficients using experimental results. Our choice of the value of $C = 0.5$ lies in the range of parameter values usually used in the literature [2,10]. We take $B = -0.625$ in Figs. 1–6 to display the behavior of the effective average potential $W_t(\phi)$ and the whole first-order phase transition process. The concrete values of B do not change the qualitative behavior of the first order phase transition. Part of the results are shown in the figures. We stop the flow when the renormalized mass term m^2 approaches a constant (Fig. 1). The stopping RG time t is roughly the same

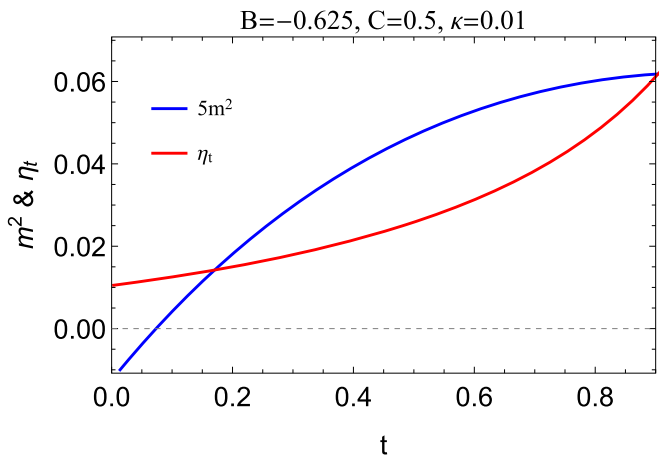

FIG. 1. Evolution of the renormalized mass and anomalous dimension with respect to RG time t.

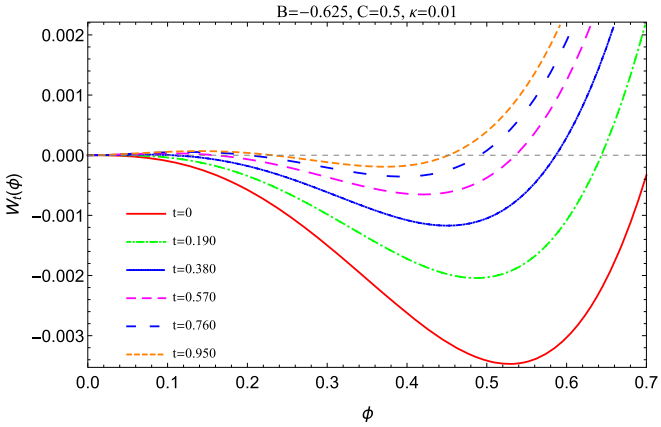

FIG. 2. Evolution of the effective average potential with respect to the field variable at different RG time t. We can see that at the end of the flow, the effective potential has two minima, one at the origin and the other at a finite value. It is clear that the one on the right-hand side stands for the physical vacuum configuration. This means that the chosen parameter $\kappa = 0.01$ corresponds to the broken symmetry phase, i.e., the nematic phase.

for the different initial κ. The running anomalous dimension (Fig. 1) is evaluated at the minimum ϕ_0 of $W_t(\phi)$. In Fig. 2 we show a typical flow of the running effective average potential. The effective potential at the end of the flow lies in the nematic phase, while the potential for a smaller κ (Fig. 3) flows into a symmetric isotropic phase. Between these two κ we can find a critical κ value that corresponds exactly to the point where the first-order phase transition happens (Fig. 4; see Fig. 5 for an enlarged portion of the end part of the flow). This is achieved through a bisection algorithm. From Fig. 5 we can read off the jump of the order parameter. We denote the effective potential at the end of the flow of $W_t(\phi)$ as $W(\phi)$. From Fig. 6 we can see clearly the whole first-order phase transition process. We have also taken a series of other parameter values of B and mapped out the order parameter

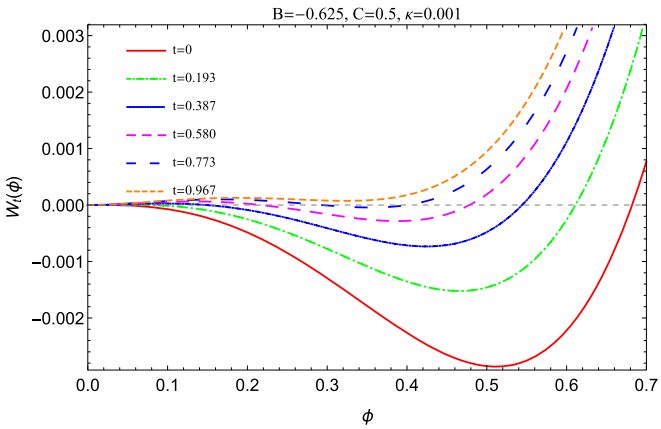

FIG. 3. Evolution of the effective average potential with respect to the field variable at different RG time t. We can see that at the end of the flow, the minimum of the effective potential that lies at the origin stands for the physical vacuum configuration. This means that the chosen parameter $\kappa = 0.001$ corresponds to the symmetric phase, i.e., the isotropic phase.

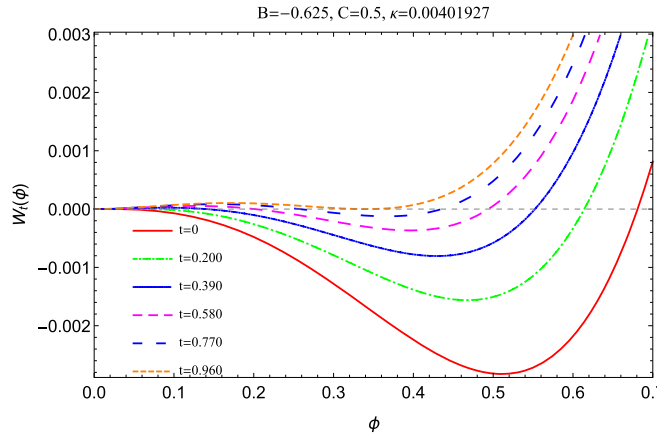

FIG. 4. From the evolution of the effective average potential for $\kappa = 0.01$ and $\kappa = 0.001$, we conclude that there must exist an intermediate value of κ that corresponds to the expected first-order phase-transition point. We find this critical value $\kappa = 0.004\,019\,27$ by using a bisection algorithm and get the evolution of the effective average potential at different RG time t for this critical κ. For an enlarged portion of the end part of the flow, see Fig. 5.

jumps following the above procedures. From Fig. 7 we can see that the order parameter jump decreases with increasing values of B. For different parameters of C we can get similar results. Given the experimental value of the order-parameter jump, we can easily extrapolate the corresponding value of B from the data in Fig. 7.

We also calculate the NI transition temperature difference to shed some light on the NI puzzle [10,13–15,32]. We follow similar techniques used in [10,13–15]. Since the first-order NI phase transition is weak and quite close to the hypothetical critical point (if there were no cubic term), as a first approximation it is reasonable to treat $\frac{t_0}{\phi^{1/\beta}}$ and $\frac{B}{\phi^{\omega}}$ as two scaling variables to get the equation of state [10,13–15,33,34]. The basic idea is that we first calculate the equation of state at $B = 0$ [i.e., the $O(5)$ model], then add a correction term that includes the effects of the symmetry-breaking term directly in the equation of state. This is also the case in Mukherjee's works [10,13–15]. According to the definition of equation of state $\frac{H}{\phi^{\delta}} = f(x)$,

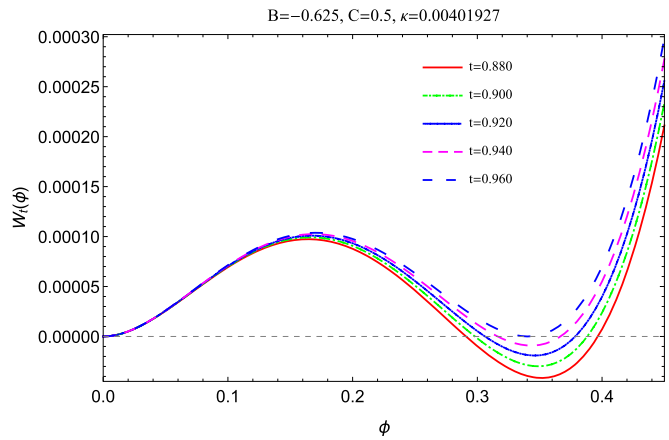

FIG. 5. Enlarged portion of the end part of the flow in Fig. 4.

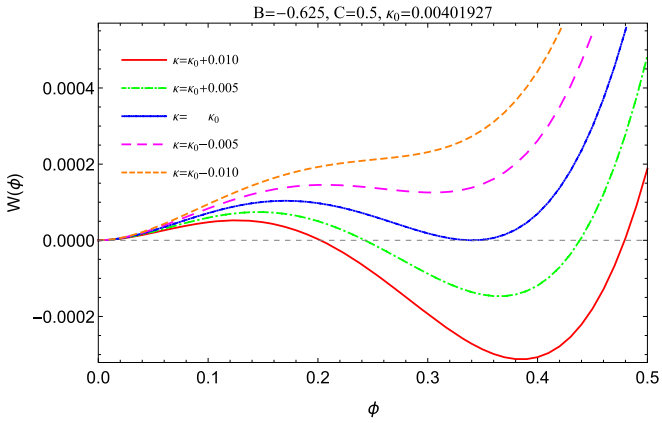

FIG. 6. Evolution of the effective potential through the first-order phase-transition point. We can see clearly the order-parameter jump. The middle touching curve corresponds to the touching curve in Fig. 5.

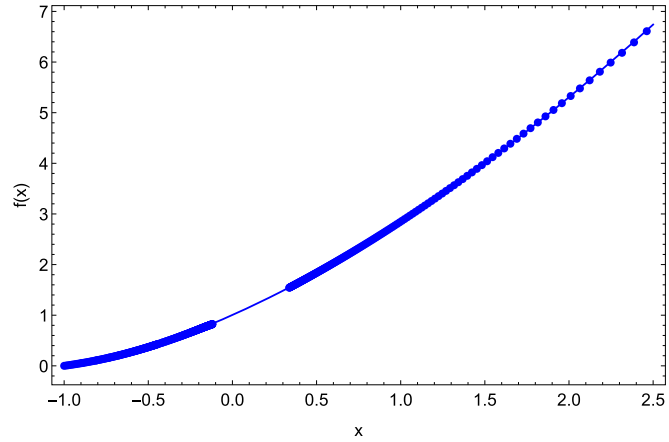

FIG. 8. Scaling function for the equation of state without the cubic term.

where H is the external field, $x = \frac{t_0}{\phi^{1/\beta}}, t_0 = \frac{T-T^*}{T^*}, \delta = \frac{D-\eta+2}{D+\eta-2}$, $\beta = \frac{1}{2}\nu(D+\eta-2)$, we follow the procedures in [26,34] and get $\nu = 0.8377$, $\eta = 0.0377$, $\beta = 0.4347$, $\delta = 4.781$ and the scaling function (Fig. 8).

$$f(x) = a(x+1)^b(c(x+1) + d\sqrt{x+1} + 1), \tag{43}$$

where $a = 0.253$, $b = 1.076$, $c = 0.221$, $d = 2.748$. We have taken the fit form of $f(x)$ used in the $O(N)$ model [26,34] and verified the above scaling relations to high accuracy. For a more detailed treatment of the equation of state of $O(N)$ model, see [26,34] and references therein. As a preliminary treatment we then add the correction term and get the approximate equation of state for Landau–de Gennes model [10,13–15]:

$$\frac{H}{\phi^\delta} + \frac{gB}{\phi^\omega} = f(x), \tag{44}$$

where and $B \sim \Delta S^\omega$ and ΔS is the jump of the order parameter. From the data in Fig. 7 we have determined the exponent $\omega = 1.10$ (for a similar result see [33]). g is to be determined later.

From thermodynamic arguments we can obtain the free energy by integrating the equation of state with respect to ϕ. Then we can express the conditions that the free energy be equal for the isotropic and nematic states and that the free energies be a local minimum with respect to ϕ as follows:

$$\int_0^{\phi_c} H(\phi')\,d\phi' = 0, \tag{45a}$$

$$H(\phi_c) = 0, \tag{45b}$$

where $\phi_c = \sqrt{\frac{2}{3}}\Delta S$, the experimental value $\Delta S = 0.4$ [10,13–15]. From the data in Fig. 7 we can easily extrapolate the value of B that corresponds to this experimental value. H can be easily solved from Eq. (44) and substituted into Eq. (45). Then we can solve the above two equations Eq. (45) for the two unknown variables t_0 and g. We get $g = 0.67$ and $t_{0c} = 0.0195$, which corresponds to the temperature difference $T_c - T^* = 5.85$ K. Although still far from the result of the experiment, our result is much smaller than the mean-field value, and about 1.5 K smaller than Mukherjee's result in [10] and about 3 K bigger than his result in [14]. This indicates that we may be on the right track to finally resolve the NI puzzle.

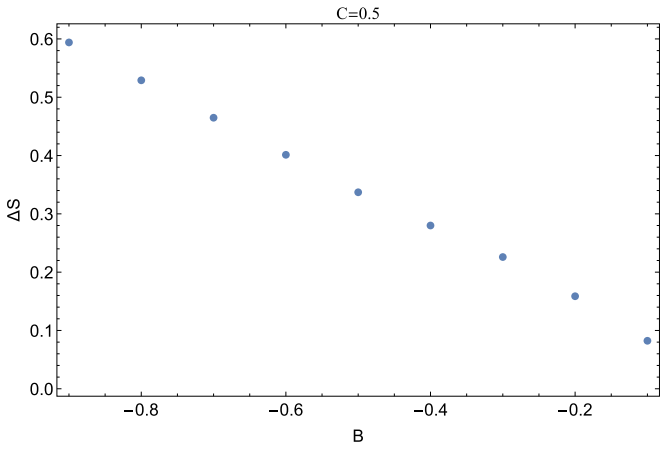

FIG. 7. The relationship between order-parameter jump ΔS and the symmetry-breaking cubic term B for $C = 0.5$.

IV. CONCLUSION

In this paper we investigate the Landau–de Gennes model in the framework of functional renormalization group. The Lagrangian density can be expanded in terms of two basic invariant combinations of the elements of the order-parameter tensor. We then solve the field variables of the order parameter in terms of the two invariants. When transformed into complex variables, the imaginary parts exactly cancel out. With the aid of Litim regulator the full analytic flow equation for the potential and its dimensionless counterpart are derived. A truncation is made to simplify the computations and we get two coupled partial differential equations for the cubic and quartic "couplings." We also derive the flow equation for the anomalous dimension. The two coupled equations are solved on a grid with the Newton-Raphson method. A large parameter space of the model is mapped and first-order phase transitions are observed.

With the experimental value of the order-parameter jump as an input, we also obtain the NI transition temperature difference. Much more interesting work can be done. For instance, we expect that a more refined and accurate analysis of the equation of state could give a better improvement. Further, our formalism can be extended to other similar models including the explicit symmetry-breaking term [35]. We leave these for future work.

ACKNOWLEDGMENTS

The work was supported in part by the Ministry of Science and Technology of China (MSTC) under the "973" Project No. 2015CB856904(4) (D.H.), and by NSFC under Grants No. 11735007 (D.H. and M.H.), No. 11375070 and No. 11521064 (D.H.), and No. 11725523 and No. 11261130311 (M.H.). H.Z. gratefully acknowledges financial support from China Scholarship Council (CSC) Grant No. 201706770051.

[1] P. G. De Gennes and J. Prost, *The Physics of Liquid Crystals* (Oxford University Press, USA, 1995).
[2] E. F. Gramsbergen, L. Longa, and W. H. de. Jeu, Phys. Rep. **135**, 195 (1986).
[3] S. Singh, Phys. Rep. **324**, 107 (2000).
[4] A. Drozd-Rzoska, S. J. Rzoska, and J. Ziolo, Phys. Rev. E **54**, 6452 (1996).
[5] A. Drozd-Rzoska, S. J. Rzoska, and J. Ziolo, Phys. Rev. E **55**, 2888 (1997).
[6] S. J. Rzoska, J. Ziolo, W. Sułkowski, J. Jadżyn, and G. Czechowski, Phys. Rev. E **64**, 052701 (2001).
[7] I. M. Syed, V. Percec, R. G. Petschek, and C. Rosenblatt, Phys. Rev. E **67**, 011704 (2003).
[8] D. S. Simeão and M. Simões, Phys. Rev. E **86**, 042701 (2012).
[9] M. Simões, D. S. Simeão, and K. E. Yamaguti, Liq. Crystallogr. **38**, 935 (2011).
[10] P. K. Mukherjee, J. Saha, B. Nandi, and M. Saha, Phys. Rev. B **50**, 9778 (1994).
[11] Z. H. Wang and P. H. Keyes, Phys. Rev. E **54**, 5249 (1996).
[12] R. Tao, P. Sheng, and Z.-F. Lin, Phys. Rev. Lett. **70**, 1271 (1993).
[13] P. K. Mukherjee and T. B. Mukherjee, Phys. Rev. B **52**, 9964 (1995).
[14] P. K. Mukherjee and M. Saha, Phys. Rev. E **51**, 5745 (1995).
[15] P. K. Mukherjee, J. Phys.: Condens. Matter **10**, 9191 (1998).
[16] C. Wetterich, Phys. Lett. B **301**, 90 (1993).
[17] K. Fukushima, K. Kamikado, and B. Klein, Phys. Rev. D **83**, 116005 (2011).
[18] Y. Jiang and P. Zhuang, Phys. Rev. D **86**, 105016 (2012).
[19] M. Grahl and D. H. Rischke, Phys. Rev. D **88**, 056014 (2013).
[20] W.-J. Fu, J. M. Pawlowski, F. Rennecke, and B.-J. Schaefer, Phys. Rev. D **94**, 116020 (2016).
[21] B. Delamotte, M. Dudka, D. Mouhanna, and S. Yabunaka, Phys. Rev. B **93**, 064405 (2016).
[22] B. Delamotte, D. Mouhanna, and M. Tissier, Phys. Rev. B **69**, 134413 (2004).
[23] A. Eichhorn, D. Mesterhazy, and M. M. Scherer, Phys. Rev. E **88**, 042141 (2013).
[24] G. Fejos, Phys. Rev. D **90**, 096011 (2014).
[25] P. Kopietz, L. Bartosch, and F. Schutz, *Introduction to the Functional Renormalization Group*, Lecture Notes in Physics, Vol. 798 (Springer, Berlin, Heidelberg, 2010).
[26] J. Berges, N. Tetradis, and C. Wetterich, Phys. Rep. **363**, 223 (2002).
[27] J. M. Pawlowski, Ann. Phys. **322**, 2831 (2007).
[28] B. Delamotte, Lect. Notes Phys. **852**, 49 (2012).
[29] W. Metzner, M. Salmhofer, C. Honerkamp, V. Meden, and K. Schonhammer, Rev. Mod. Phys. **84**, 299 (2012).
[30] D. F. Litim, Phys. Rev. D **64**, 105007 (2001).
[31] J. A. Adams, J. Berges, S. Bornholdt, F. Freire, N. Tetradis, and C. Wetterich, Mod. Phys. Lett. A **10**, 2367 (1995).
[32] R. G. Priest, Mol. Cryst. Liq. Cryst. **41**, 223 (1978).
[33] J. Berges and C. Wetterich, Nucl. Phys. B **487**, 675 (1997).
[34] J. Braun and B. Klein, Phys. Rev. D **77**, 096008 (2008).
[35] M. Kindermann and C. Wetterich, Phys. Rev. Lett. **86**, 1034 (2001).